Differential *Tks5* isoform expression contributes to metastatic invasion of lung adenocarcinoma

Carman Man-Chung Li,[1] Guoan Chen,[2] Talya L. Dayton,[1] Caroline Kim-Kiselak,[1] Sebastian Hoersch,[1] Charles A. Whittaker,[1] Roderick T. Bronson,[3] David G. Beer,[2] Monte M. Winslow,[4] and Tyler Jacks[1,5,6]

[1]David H. Koch Institute for Integrative Cancer Research, Department of Biology, Massachusetts Institute of Technology, Cambridge, Massachusetts 02139, USA; [2]Department of Surgery, Thoracic Surgery, University of Michigan Medical School, Ann Arbor, Michigan 48109, USA; [3]Department of Pathology, Tufts University School of Medicine and Veterinary Medicine, North Grafton, Massachusetts 01536, USA; [4]Department of Genetics, Stanford University School of Medicine, Stanford, California 94305, USA; [5]Howard Hughes Medical Institute, Massachusetts Institute of Technology, Cambridge, Massachusetts 02139, USA

Metastasis accounts for the vast majority of cancer-related deaths, yet the molecular mechanisms that drive metastatic spread remain poorly understood. Here we report that *Tks5*, which has been linked to the formation of proteolytic cellular protrusions known as invadopodia, undergoes an isoform switch during metastatic progression in a genetically engineered mouse model of lung adenocarcinoma. Nonmetastatic primary tumor-derived cells predominantly expressed a short isoform, $Tks5_{short}$, while metastatic primary tumor- and metastasis-derived cells acquired increased expression of the full-length isoform $Tks5_{long}$. This elevation of $Tks5_{long}$ to $Tks5_{short}$ ratio correlated with a commensurate increase in invadopodia activity in metastatic cells compared with nonmetastatic cells. Further characterization of these isoforms by knockdown and overexpression experiments demonstrated that $Tks5_{long}$ promoted invadopodia in vitro and increased metastasis in transplant models and an autochthonous model of lung adenocarcinoma. Conversely, $Tks5_{short}$ decreased invadopodia stability and proteolysis, acting as a natural dominant-negative inhibitor to $Tks5_{long}$. Importantly, high $Tks5_{long}$ and low $Tks5_{short}$ expressions in human lung adenocarcinomas correlated with metastatic disease and predicted worse survival of early stage patients. These data indicate that tipping the *Tks5* isoform balance to a high $Tks5_{long}$ to $Tks5_{short}$ ratio promotes invadopodia-mediated invasion and metastasis.

[*Keywords*: Tks5; invadopodia; metastasis; lung adenocarcinoma; non-small-cell lung cancer; mouse model]

Supplemental material is available for this article.

Received October 18, 2012; revised version accepted June 19, 2013.

Despite the high rates of mortality associated with metastatic lung cancer (Keshamouni et al. 2009; Siegel et al. 2013), the molecular mechanisms underlying disease progression remain incompletely understood. Metastasis accounts for the vast majority of all lung cancer fatalities, as even 30%–50% of early stage patients who undergo surgical resection eventually succumb to metastatic relapse, and patients with metastatic disease are almost always incurable (Keshamouni et al. 2009). The development of more effective therapeutic interventions for this disease will rely on improving our understanding of metastasis at the molecular level.

Tks5 (also known as *Sh3pxd2a*) has been previously implicated in promoting metastasis because of its role in invasive cellular structures known as invadopodia (Courtneidge 2012). Invadopodia are actin-rich, proteolytic membrane protrusions that were initially identified in Src-transformed mouse embryonic fibroblasts (Chen et al. 1984; Tarone et al. 1985) and later observed in a variety of cultured human cancer cells, including breast cancer, melanoma, and head and neck squamous cell carcinoma (Seals et al. 2005; Bowden et al. 2006; Clark et al. 2007). While invadopodia formation is spontaneous in some cancer cells in culture, it can be further stimulated by activating integrin β1 and receptors for epidermal growth factor (EGF) and platelet-derived growth factor (PDGF) (Nakahara et al. 1998; Yamaguchi et al. 2005; Philippar et al. 2008; Eckert et al. 2011). These cellular "invasive feet" have been demonstrated to produce a variety of proteases, including metalloproteases (MMP2, MMP9, MT1-MMP, and the ADAM family of sheddases) and serine proteases (seprase and uPAR) (Linder 2007), and are capable of digesting various components of the extracellular matrix in vitro (Kelly et al. 1994). Given their proteolytic

[6]**Corresponding author**
E-mail tjacks@mit.edu
Article is online at http://www.genesdev.org/cgi/doi/10.1101/gad.222745.113.

capabilities, invadopodia are thought to facilitate metastasis by enabling tumor cells to breach the basement membrane, degrade the extracellular matrix, and invade into the stroma during the intravasation and extravasation steps of the metastatic cascade (Murphy and Courtneidge 2011). In fact, it has been proposed that invadopodia in cancer cells are a co-opted and dysregulated version of normal cellular structures known as podosomes that are found in untransformed cells such as osteoclasts, macrophages, dendritic cells, endothelial cells, and smooth muscle cells (Murphy and Courtneidge 2011). Although it is still unclear whether invadopodia have any physiological function in metastatic invasion during natural tumor progression (Linder 2009; Sibony-Benyamini and Gil-Henn 2012), animal transplant studies and intravital imaging have provided some in vivo evidence for a role for invadopodia in mediating metastasis (Philippar et al. 2008; Gligorijevic et al. 2012).

Tks5 is an important component of invadopodia and mediates invadopodia formation by acting as a Src-dependent scaffolding protein (Lock et al. 1998). Upon phosphorylation by Src, the N-terminal phox (PX) homology domain of Tks5 is thought to be released from intramolecular interactions and becomes free to bind membrane phosphoinositides, including PI(3,4)P2, thereby localizing Tks5 to the site of invadopodia formation (Abram et al. 2003; Oikawa et al. 2008). Tks5 also contains five C-terminal Src homology 3 (SH3) domains, which recruit effector proteins (including AFAP-110, cortactin, and ADAM metalloproteases) to initiate actin polymerization and matrix degradation (Abram et al. 2003; Crimaldi et al. 2009). Knockdown of *Tks5* (targeting all isoforms simultaneously) abrogates invadopodia formation and proteolytic function in cultured human breast cancer and melanoma cells (Seals et al. 2005) and reduces lung metastasis formation by Src-transformed NIH-3T3 mouse embryonic fibroblasts and Ras-transformed human mammary epithelial cells after intravenous injection or subcutaneous transplantation (Blouw et al. 2008; Eckert et al. 2011).

Despite the evidence that *Tks5* is important for invadopodia formation in cell lines, its contribution to the metastatic process in naturally evolving tumors has not been elucidated. Moreover, previous studies have not accounted for the presence of the two functionally distinct isoforms (which we termed $Tks5_{long}$ and $Tks5_{short}$) that we characterize in this study. These two *Tks5* variants were first detected by immunoblotting in Src-transformed NIH-3T3 cells when *Tks5* was initially identified (Lock et al. 1998); however, no subsequent functional studies have taken into account the existence of these isoforms. Therefore, the distinct roles of $Tks5_{long}$ and $Tks5_{short}$ in invadopodia function and cancer invasion are unknown.

Here we report that $Tks5_{long}$ and $Tks5_{short}$ play distinct and opposing roles in regulating invadopodia-mediated invasion in lung adenocarcinoma. We show that metastatic primary tumor- and metastasis-derived cells acquired an elevated ratio of $Tks5_{long}$ to $Tks5_{short}$ expression and a commensurate increase in invadopodia activity compared with nonmetastatic cells. We further demonstrate that the ratio of $Tks5_{long}$ to $Tks5_{short}$ expression regulates invadopodia function in vitro and influences metastatic potential in transplant models and a genetically engineered mouse model of lung cancer. Finally, we provide evidence that the relative expression of $Tks5_{long}$ and $Tks5_{short}$ represents an important prognostic factor in human lung cancer. These results highlight the isoform-dependent roles of *Tks5* in invadopodia and metastasis.

Results

Metastatic and nonmetastatic lung adenocarcinoma cells exhibit differential expression of $Tks5_{long}$ *and* $Tks5_{short}$

To better characterize the cell state changes and molecular alterations that accompany tumor progression and metastasis in lung adenocarcinoma, we recently developed a $K\text{-}ras^{LSL\text{-}G12D/WT}; p53^{flox/flox}$ mouse model for studying metastatic and nonmetastatic primary tumors (Winslow et al. 2011). This model harbors genetic mutations frequently found in human lung adenocarcinoma (Rodenhuis et al. 1988; Takahashi et al. 1989) and closely recapitulates the histopathological progression of the human disease (Jackson et al. 2005). Although these mice develop multiple $K\text{-}ras^{G12D}$, $p53^{-/-}$ lung tumors after inhalation of lentivirus expressing Cre recombinase, only a subset of tumors eventually acquire full metastatic potential, suggesting that progression to metastasis requires additional genetic and/or epigenetic events. Importantly, this model allows the identification of metastatic versus nonmetastatic primary tumors, as the metastases that form in these mice can be matched to their primary tumor of origin based on the common lentiviral integration site in their genome. Thus, primary tumors (T_{Met}) that have given rise to metastatic lesions can be distinguished from primary tumors for which no metastasis was found (T_{nonMet}). Cell lines derived from these T_{Met} and T_{nonMet} tumors were examined for their gene expression profiles via exon microarrays, which identified expression alterations in various genes, including Nkx2-1 and Hmga2, that were associated with metastatic progression (Winslow et al. 2011).

To identify gene isoform expression changes that could be caused by alternative splicing or differential promoter utilization in our collection of autochthonous tumor-derived T_{nonMet} and T_{Met} cells, we developed an algorithm that allowed us to query our exon array data for changes in isoform usage. The most striking result from this analysis was a change in *Tks5* isoform expression between T_{nonMet} and T_{Met} cells (Supplemental Fig. S2). We identified two *Tks5* isoforms by referencing sequences published on the University of California at Santa Cruz genome browser (http://genome.ucsc.edu, assembly NCBI37/mm9, gene *Sh3pxd2a*): $Tks5_{long}$, which contains exons 1–15, and $Tks5_{short}$, which contains a distinct 5′ sequence from intron 7 followed by exons 8–15 (Fig. 1A). Both transcripts encode five SH3 domains in the C terminus, but only $Tks5_{long}$ contains the N-terminal PX homology domain (Fig. 1A).

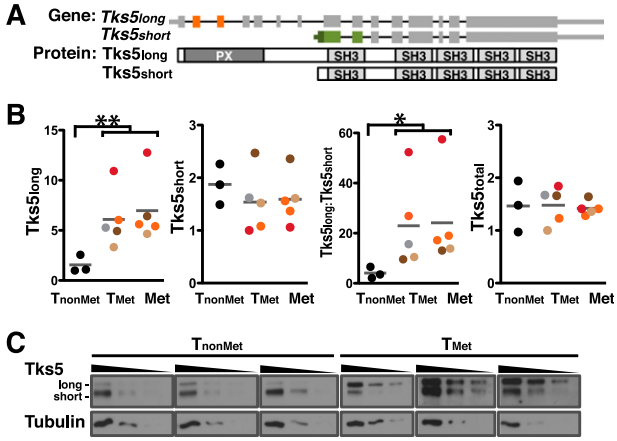

Figure 1. T_{nonMet} and T_{Met} lung adenocarcinoma cells exhibit differential expression of *Tks5*$_{long}$ and *Tks5*$_{short}$. (*A*) *Tks5*$_{long}$ and *Tks5*$_{short}$ differ in their 5′ coding sequences and hence the presence of the N-terminal PX homology domain in the encoded proteins. The 3′ coding sequence common in the *Tks5*$_{long}$ and *Tks5*$_{short}$ transcripts encodes five SH3 domains in the C terminus of the protein. (*B*) Isoform-specific qRT–PCR analysis of *Tks5*$_{long}$ and *Tks5*$_{short}$ expression in three T_{nonMet} (368T1, 394T4, and 802T4), five T_{Met} (373T1, 389T2, 393T3, 393T5, and 482T1), and five Met (373N1, 393N1, 393M1, 482N1, and 482M1) cell lines. Color dots indicate matching T_{Met} and Met cell lines in the same lineage. (Red) 373T1 and 373N1; (brown) 393T3 and 393N1; (beige) 393T5 and 393M1; (orange) 482T1, 482N1, and 482M1. N indicates lymph node metastasis, while M indicates distant metastasis. *Tks5*$_{long}$-specific primers amplify exons 2 and 3 (indicated in orange in *A*), while *Tks5*$_{short}$-specific primers amplify a *Tks5*$_{short}$-unique 5′ sequence and exons 8 and 9 (indicated in green in *A*). (**) *P*-value < 0.01; (*) *P*-value < 0.05, Student's *t*-test. (*C*) Immunoblot detection of Tks5 isoforms in a serial dilution of three T_{nonMet} (368T1, 394T4, and 802T4) and three T_{Met} (373T1, 393T3, and 482T1) cell lysates. Tubulin was used as a loading control.

We confirmed the differential expression of *Tks5*$_{long}$ and *Tks5*$_{short}$ in T_{nonMet} and T_{Met} cells by performing isoform-specific quantitative RT–PCR (qRT–PCR) on a panel of three T_{nonMet} cell lines as well as five T_{Met} cell lines and their five matching metastasis cell lines (Met). Consistent with the microarray data, *Tks5*$_{long}$ transcript levels were, on average, fourfold higher in T_{Met}/Met cells compared with T_{nonMet} cells, while *Tks5*$_{short}$ was transcribed at a similar level between T_{Met}/Met and T_{nonMet} cells (Fig. 1B). As a result, the ratio of *Tks5*$_{long}$ to *Tks5*$_{short}$ was, on average, sixfold higher in T_{Met}/Met cells than T_{nonMet} cells (Fig. 1B). Consistent with the mRNA expression patterns, the ratio of $Tks5_{long}$ to $Tks5_{short}$ proteins (150 kDa and 140 kDa, respectively) is higher in T_{Met} cells compared with T_{nonMet} cells (Fig. 1C).

Interestingly, despite this increase in *Tks5*$_{long}$ transcripts, because *Tks5*$_{long}$ only accounted for a fraction of total *Tks5* expression, the levels of total *Tks5* transcript did not vary significantly between T_{nonMet} and T_{Met}/Met cell lines in our exon microarray or in our qRT–PCR analysis using primers targeting a common region shared by *Tks5*$_{long}$ and *Tks5*$_{short}$ transcripts (Fig. 1B). Thus, the T_{nonMet} and T_{Met}/Met cell lines could be distinguished by their *Tks5*$_{long}$ expression or *Tks5*$_{long}$ to *Tks5*$_{short}$ ratio but not by total *Tks5* level. 5′ RACE and H3K4me3 chromatin immunoprecipitation sequencing (ChIP-seq) analyses suggest that the two isoforms are transcribed from distinct promoters (data not shown).

Expression of $Tks5_{long}$ *and* $Tks5_{short}$ *in* T_{nonMet} *and* T_{Met} *cells correlates with invadopodia formation and function*

Given the differences in *Tks5* isoform levels between T_{Met} and T_{nonMet} cells and the previously reported role of *Tks5* in mediating invadopodia activity, we compared three T_{nonMet} and four T_{Met} cell lines for invadopodia formation and function. To measure invadopodia formation, we performed immunofluorescence staining to detect the colocalization of two essential invadopodia components: cortactin and F-actin (Fig. 2A). T_{Met} cells, which have a higher *Tks5*$_{long}$ to *Tks5*$_{short}$ ratio, displayed

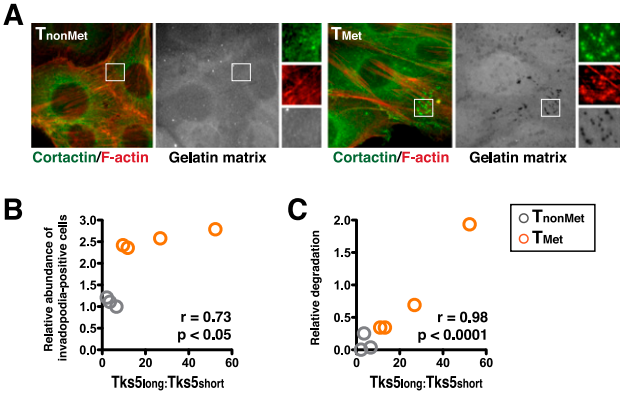

Figure 2. Differential *Tks5*$_{long}$ and *Tks5*$_{short}$ expression in T_{nonMet} and T_{Met} lung adenocarcinoma cells correlates with invadopodia formation and function. (*A*) Colocalization of invadopodia components cortactin (green) and F-actin (red) as well as FITC-negative areas of gelatin degradation are more readily observed in T_{Met} cells compared with T_{nonMet} cells. Cells were cultured on a thin layer of FITC-labeled gelatin for 24 h and then fixed and processed for immunofluorescence staining. Magnified views of the regions indicated by the boxed area are shown at the *right*. Representative images of T_{nonMet} and T_{Met} cells are shown. (*B*) Correlation between invadopodia formation and the ratio of *Tks5*$_{long}$ to *Tks5*$_{short}$ expression in three T_{nonMet} cell lines (gray circles; specifically, 368T1, 394T4, and 802T4 from *left* to *right*) and four T_{Met} cell lines (orange circles; specifically, 393T3, 393T5, 482T1, and 373T1 from *left* to *right*). Cells with colocalization of cortactin and F-actin in immunofluorescence staining were scored as invadopodia-positive. At least 60 cells were scored for each cell line. Results are representative of three independent experiments. (*C*) Correlation between gelatin matrix degradation and the ratio of *Tks5*$_{long}$ to *Tks5*$_{short}$ expression in three T_{nonMet} cell lines (gray circles; specifically, 368T1, 394T4, and 802T4 from *left* to *right*) and four T_{Met} cell lines (orange circles; specifically, 393T3, 393T5, 482T1, and 373T1 from *left* to *right*). Areas of degradation were quantified using ImageJ and normalized to number of cells per field. At least 50 fields and 1500 cells were analyzed per cell line. Results are representative of three independent experiments.

a higher frequency of colocalized cortactin and F-actin than T_{nonMet} cells (Fig. 2B). To measure invadopodia function, we examined invadopodia-mediated proteolysis in T_{nonMet} and T_{Met} cells by culturing them on a thin layer of FITC-labeled gelatin. The degraded areas can be observed by fluorescence microscopy as FITC-negative patches that frequently coincide with cortactin/F-actin-stained invadopodia foci (Fig. 2A). The gelatin degradation assay is a more sensitive method to measure invadopodia activity compared with cortactin/F-actin immunofluorescence staining because the effect of degradation is cumulative over time, while the presence of invadopodia is transient. Quantification of the degradation area showed a strong correlation between the proteolytic capability of these T_{nonMet} and T_{Met} cells and their ratio of *Tks5*$_{long}$ to *Tks5*$_{short}$ expression: T_{Met} cells with higher *Tks5*$_{long}$ to *Tks5*$_{short}$ ratios were more proteolytic on the gelatin matrix compared with T_{nonMet} cells (Fig. 2C). Importantly, we did not observe significant differences in other invadopodia components at either the total gene expression or isoform level by exon array analysis (analyzed for Tks4, Src, Cortactin, Afap110, p190 RhoGAP, Arg, N-WASP, Arp2/3 complex subunits, Wave1, Cdc42, Cofilin, Gelsolin, MT1-MMP, MMP2, MMP9, ADAM12, ADAM15, and ADAM19) or the protein phosphorylation level by Western blot (analyzed for Src) (data not shown). Taken together, these observations suggest that an increased ratio of *Tks5*$_{long}$ to *Tks5*$_{short}$ is associated with the enhanced invadopodia formation and function that we observed in T_{Met} cells compared with T_{nonMet} cells.

Knockdown of Tks5$_{long}$ *impairs invadopodia activity and metastasis formation*

Since the distinct functions of *Tks5*$_{long}$ and *Tks5*$_{short}$ in invadopodia have not been previously reported, we tested whether *Tks5*$_{long}$ was specifically required for invadopodia formation and function in two T_{Met} cell lines. Stable RNAi-mediated depletion of *Tks5*$_{long}$ using two isoform-specific shRNAs reduced *Tks5*$_{long}$ expression in T_{Met} cells by 55%–65% without a significant effect on *Tks5*$_{short}$ (Fig. 3A,B). *Tks5*$_{long}$ knockdown impaired the ability of T_{Met} cells to form invadopodia as measured by immunofluorescence staining for cortactin/F-actin foci (Fig. 3C,D; Supplemental Fig. S3A,B). These T_{Met}-*shTks5*$_{long}$ cells also exhibited significantly reduced extracellular matrix proteolysis capability when cultured on FITC gelatin (Fig. 3C,E; Supplemental Fig. S3A,C). Because these observations were consistent for both *shTks5*$_{long}$ shRNAs, it is unlikely that they were the results of off-target effects. Collectively, these data indicate that *Tks5*$_{long}$ is necessary for invadopodia activity in metastatic lung cancer cells.

To determine whether the effects of *Tks5*$_{long}$ knockdown on invadopodia activity in vitro translate to the inhibition of metastatic ability in vivo, we transplanted T_{Met}-sh*Tks5*$_{long}$ cells subcutaneously into athymic nude mice to assess the metastatic potential of tumor cells. T_{Met} cells with *Tks5*$_{long}$ knockdown exhibited a significantly diminished ability to disseminate from the

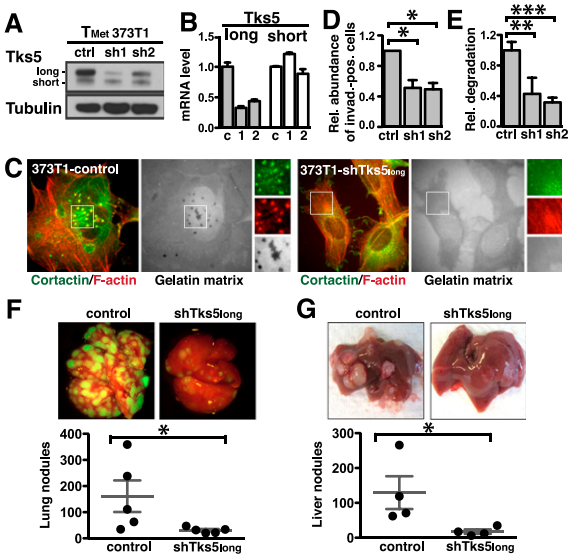

Figure 3. *Tks5*$_{long}$ is required for invadopodia activity in vitro and metastasis formation in vivo. (*A*) Immunoblot detection of Tks5 isoforms in T_{Met} cells (373T1) expressing control shRNA (shLuciferase) or *Tks5*$_{long}$-specific shRNAs (sh1 and sh2). Tubulin was used as a loading control. (*B*) qRT–PCR analysis shows that sh1 and sh2 reduce *Tks5*$_{long}$ transcripts by 55%–65% without significant effects on *Tks5*$_{short}$ mRNA levels. (*C*) Immunofluorescence staining shows that colocalization of invadopodia components (cortactin is in green, and F-actin is in red) and FITC-negative areas of gelatin matrix degradation are less frequently observed in T_{Met}-sh*Tks5*$_{long}$ cells compared with T_{Met} cells expressing control shRNA. Magnified views of the regions indicated by the boxed area are shown to the *right*. Representative images from T_{Met} cells (373T1) are shown. (*D*) Effects of *Tks5*$_{long}$ knockdown on invadopodia formation in T_{Met} cells (373T1). At least 100 cells were scored for colocalization of cortactin and F-actin in three independent experiments. All values are mean ± SEM. (*) *P*-value < 0.05, paired *t*-test. (*E*) Effects of *Tks5*$_{long}$ knockdown on FITC gelatin matrix degradation in T_{Met} cells (373T1). Areas of degradation were quantified using ImageJ and normalized to number of cells per field. At least 75 fields containing a total of 600 cells were analyzed per condition. All values are mean ± SEM. (**) *P*-value < 0.01; (***) *P*-value < 0.001, Student's *t*-test. (*F*) *Tks5*$_{long}$ knockdown drastically impairs lung nodule formation 8 wk after subcutaneous transplant of GFP-positive T_{Met} cells (393T3). Values are mean ± SEM; *P* < 0.05, Student's *t*-test. (*G*) *Tks5*$_{long}$ knockdown significantly decreases liver nodule formation 3 wk after intrasplenic transplant of T_{Met} cells (373T1). Values are mean ± SEM; *P* < 0.05, Student's *t*-test.

subcutaneous site and form lung tumor nodules compared with parental cells 8 wk after subcutaneous injection (Fig. 3F). Of note, the sizes of the subcutaneous tumors were comparable between the two mouse cohorts, suggesting that loss of *Tks5*$_{long}$ expression had no effect on primary tumor growth (Supplemental Fig. S3D). Furthermore, in a separate experiment, we transplanted cells intrasplenically to assess their ability to extravasate and colonize the liver after draining into the hepatic portal vein from the spleen. Consistent with data from the subcutaneous transplant experiment, intrasplenically

injected T_{Met}-*shTks5*$_{long}$ cells showed a substantially reduced ability to form liver nodules 3 wk after transplantation compared with controls (Fig. 3G). Importantly, inefficient liver colonization by T_{Met}-*shTks5*$_{long}$ cells was not a result of reduced cell proliferation or increased apoptosis, as the infrequent liver nodules that were formed by T_{Met}-*shTks5*$_{long}$ cells displayed similar mitotic and apoptotic indices compared with parental cells (Supplemental Fig. S3E,F). These experiments suggest that *Tks5*$_{long}$-induced invadopodia are not only important for promoting cell invasion during intravasation at the primary site, but also required for extravasation and/or colonization at the metastatic sites, potentially by facilitating metastatic cell exit from blood vessels and/or invasion at secondary sites.

Increased $Tks5_{long}$ *expression promotes invadopodia activity and metastasis formation*

To ask whether exogenous expression of *Tks5*$_{long}$ alone is sufficient to enhance invadopodia formation and function in T_{nonMet} cells, we generated a lentivirus that allows doxycycline-inducible expression of Flag-tagged *Tks5*$_{long}$ (Fig. 4A). Increased expression of *Tks5*$_{long}$ in two independent T_{nonMet} cell lines promoted invadopodia formation compared with parental cells as measured by immunofluorescence staining for foci of cortactin/F-actin colocalization (Fig. 4B,C; Supplemental Fig. S4A). Moreover, these cells also displayed a dramatic sixfold to 14-fold increase in matrix proteolysis in the FITC gelatin degradation assay (Fig. 4B,D; Supplemental Fig. S4B). Our data thus demonstrate that changing the *Tks5*$_{long}$ to *Tks5*$_{short}$ ratio by increasing *Tks5*$_{long}$ expression is sufficient to promote invadopodia formation and function in nonmetastatic lung adenocarcinoma cells.

We then sought to determine whether *Tks5*$_{long}$ also facilitates tumor metastasis in vivo. To test this in a physiologically relevant model of tumor progression, we infected *K-ras*$^{LSL\text{-}G12D/WT}$; *p53*$^{flox/flox}$; *Rosa26-LSL-TdTomato; CCSP-rtTA* mice with a PGK-Cre/TRE-*Tks5*$_{long}$ lentivirus (Fig. 4E). Inhalation of the virus initiates RFP-positive lung tumors through the concomitant activation of oncogenic *K-ras* and deletion of *p53*. Infected mice were then fed with a doxycycline diet starting at 4 wk post-infection to induce Flag-tagged *Tks5*$_{long}$ expression, allowing us to study the effects of *Tks5*$_{long}$ specifically on tumor progression and not initiation. We confirmed inducible expression of our construct through detection of doxycycline- and rtTA-dependent expression of Flag-tagged *Tks5*$_{long}$ in these lung tumors (Supplemental Fig. S4C). At 6 mo post-infection, although widespread distant metastases had not yet developed, we observed a significant acceleration in primary tumor progression in *Tks5*$_{long}$ mice ($n = 9$ mice; 221 tumors) compared with the control mice ($n = 14$ mice; 397 tumors): *Tks5*$_{long}$ tumors had a smaller proportion of low-grade tumors and a commensurate increase in high-grade lesions (Supplemental Fig. S4D). These high-grade tumors were invasive into stromal tissues surrounding the blood vessels and were thus categorized as grade 4 lesions (Supplemental Fig. S4E).

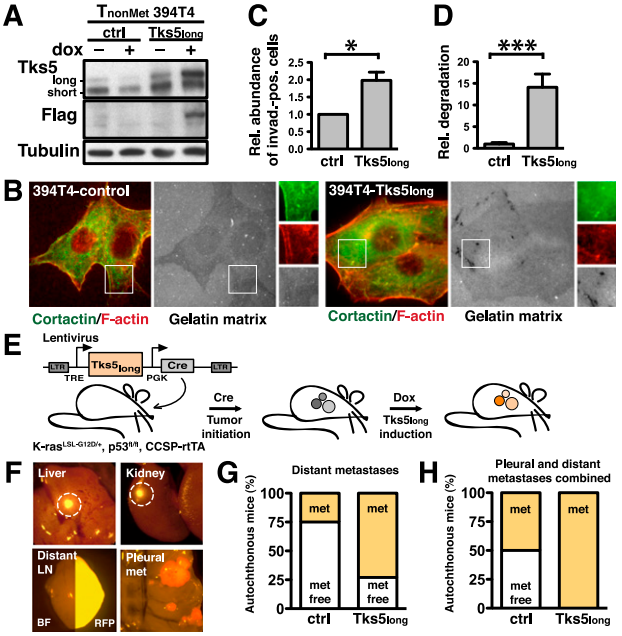

Figure 4. *Tks5*$_{long}$ is sufficient to promote invadopodia activity in vitro and metastasis formation in vivo. (*A*) Immunoblot detection of Tks5 isoforms in 394T4 T_{nonMet} cells and T_{nonMet}-Flag-*Tks5*$_{long}$ cells with or without doxycycline induction of Flag-*Tks5*$_{long}$. Tubulin was used as a loading control. (*B*) Immunofluorescence staining shows that colocalization of invadopodia components (cortactin is in green, and F-actin is in red) and FITC-negative areas of gelatin matrix degradation are more readily observed in T_{nonMet}-*Tks5*$_{long}$ cells compared with parental T_{nonMet} cells, both treated with 2 μg/mL doxycycline. Magnified views of the regions indicated by the boxed area are shown at the *right*. Representative images of T_{nonMet} cells (394T4) are shown. (*C*) Effects of increased *Tks5*$_{long}$ expression on invadopodia formation in T_{nonMet} cells (394T4). At least 100 cells were scored for colocalization of cortactin and F-actin in three independent experiments. All values are mean ± SEM. (*) *P*-value < 0.05, paired *t*-test. (*D*) Effects of increased *Tks5*$_{long}$ expression on FITC gelatin matrix degradation in T_{nonMet} cells (394T4). Areas of degradation were quantified using ImageJ and normalized to number of cells per field. At least 40 fields containing a total of 1800 cells were analyzed per condition. All values are mean ± SEM. (***) *P*-value < 0.001, Student's *t*-test. (*E*) Induction of lung adenocarcinomas with doxycycline-dependent overexpression of *Tks5*$_{long}$ in an autochthonous mouse model. *K-ras*$^{LSL\text{-}G12D/WT}$; *p53*$^{flox/flox}$; *CCSP-rtTA* mice were infected with a PGK-Cre/TRE-*Tks5*$_{long}$ lentivirus. The Cre recombinase initiates lung adenocarcinomas upon infection. Doxycycline diet later induced *Tks5*$_{long}$ expression in these tumors to study the effects of *Tks5*$_{long}$ on tumor progression without affecting tumor initiation. (*F*) Examples of distant metastases observed in mice with increased *Tks5*$_{long}$ expression. All tumors are RFP-positive because of a *Rosa26-LSL-TdTomato* allele in the mice. (BF) Bright field. (*G*) Mice with increased *Tks5*$_{long}$ expression ($n = 15$) developed more distant metastases compared with control mice ($n = 8$). $P < 0.03$, χ^2 test; $P < 0.04$, Fisher's exact test, two tailed. (*H*) Mice with increased *Tks5*$_{long}$ expression ($n = 15$) developed more metastases overall (including distant metastases and pleural metastases) compared with control mice ($n = 8$). $P < 0.003$, χ^2 test; $P < 0.008$, Fisher's exact test, two tailed.

Consistent with these observations, at 8 mo post-infection, when mice had developed both pleural metastases and distant metastases in the liver, kidneys, and distant lymph nodes (Fig. 4F), $Tks5_{long}$-expressing mice developed significantly more distant metastases (11 of 15 mice) than the control group (two of eight mice; $P < 0.05$ by both χ^2 test and Fisher's exact test) (Fig. 4G). In addition, 15 of 15 $Tks5_{long}$ mice developed pleural metastases and/or distant metastases, while four of eight mice in the control group remained metastasis-free ($P < 0.003$ by χ^2 test and $P < 0.008$ by Fisher's exact test) (Fig. 4H). Importantly, we did not observe any significant difference in the primary lung tumor sizes and total lung tumor burden in the $Tks5_{long}$ mice versus control mice (Supplemental Fig. S4F,G), suggesting that the effect of $Tks5_{long}$ on tumor progression and metastasis was not a consequence of increasing the rate of tumor growth.

Collectively, these data from this mouse model indicate that $Tks5_{long}$ plays an important role in promoting metastasis in vivo and are consistent with our in vitro evidence that $Tks5_{long}$ promotes invadopodia-mediated invasion. Whether tumor progression can be further stimulated by other mechanisms—including, for example, growth factor shedding during invadopodia-mediated degradation of the extracellular matrix—remains an open possibility and will be addressed in future studies.

Elevated expression of $Tks5_{short}$ *reduces gelatin matrix degradation and invadopodia lifetime*

In addition to modulating $Tks5_{long}$ expression, the $Tks5_{long}$ to $Tks5_{short}$ ratio can also be altered by increasing the expression of the less well-studied isoform $Tks5_{short}$. While $Tks5_{short}$ levels in T_{nonMet} and T_{Met}/Met cells were similar, we were interested whether $Tks5_{short}$ could also participate in regulating invadopodia activity. Although we attempted to knock down $Tks5_{short}$ by shRNA, this approach proved to be challenging, since the unique sequence in the $Tks5_{short}$ transcript is very short. Therefore, we chose to infect T_{Met} cells with a lentivirus that allowed doxycycline-inducible expression of HA-tagged $Tks5_{short}$ (Fig. 5A). Interestingly, two independent T_{Met} cell lines with exogenous $Tks5_{short}$ expression both had drastically reduced gelatin matrix proteolysis (Fig. 5B), suggesting that $Tks5_{short}$ may act in a dominant-negative manner over $Tks5_{long}$ in regulating invadopodia activity.

We additionally determined the localization of $Tks5_{short}$ by using an antibody specific for the HA tag and found that HA-$Tks5_{short}$ exhibited a diffuse localization in T_{Met}-$Tks5_{short}$ cells (Fig. 5C). This distribution is in contrast to that of endogenous Tks5 in T_{Met} cells stained with a pan-Tks5 antibody, where the protein (presumably the dominant $Tks5_{long}$ isoform in T_{Met} cells) is concentrated at foci of cortactin/F-actin colocalization (Fig. 5C). The diffuse distribution of $Tks5_{short}$ suggests that it cannot localize to invadopodia foci on the cell membrane, conceivably due to lack of a PX homology domain.

Moreover, even though cortactin/F-actin-positive foci of invadopodia could be observed in T_{Met}-$Tks5_{short}$ cells

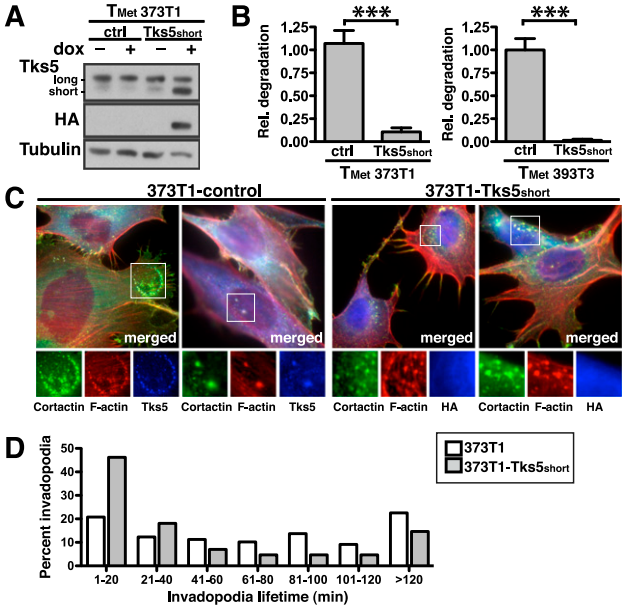

Figure 5. $Tks5_{short}$ negatively regulates extracellular matrix degradation and reduces invadopodia lifetime. (*A*) Immunoblot detection of Tks5 isoforms in 373T1 T_{Met} cells and T_{Met}-HA-$Tks5_{short}$ cells with or without doxycycline induction of HA-$Tks5_{short}$ expression. Tubulin was used as a loading control. (*B*) Increased expression of $Tks5_{short}$ in two independent T_{Met} cell lines (373T1 and 393T3) impairs gelatin matrix proteolysis. Both T_{Met}-$Tks5_{short}$ cells and parental T_{Met} cells were treated with 2 μg/mL doxycycline. Areas of degradation were quantified using ImageJ and normalized to number of cells per field. At least 40 fields containing a total of 1300 cells were analyzed per condition. Values are mean ± SEM; (***) *P*-value < .001, Student's *t*-test. (*C*) Immunofluorescence staining of total Tks5 in 373T1 T_{Met} cells and of HA-$Tks5_{short}$ in 373T1 T_{Met}-HA-$Tks5_{short}$ cells, both treated with 2 μg/mL doxycycline. Invadopodia were stained by its components (cortactin is in green, and F-actin is in red). Magnified views of the regions indicated by the boxed area are shown at the *right*. Representative images are shown. (*D*) Invadopodia lifetime in 373T1 T_{Met}-$Tks5_{short}$ cells are generally shorter than control 373T1 T_{Met} cells as measured by live cell fluorescence imaging. More than 150 invadopodia from three independent measurements were analyzed per condition.

(Fig. 5C), when we measured the lifetime of invadopodia in these cells using time-lapse fluorescence imaging, they exhibited shortened invadopodia lifetime compared with parental T_{Met} cells (Fig. 5D). Previous studies have shown that nascent invadopodia remain nonproteolytic for at least 1 h before maturing into fully functional invadopodia that are capable of mediating degradation (Yamaguchi et al. 2005; Oser et al. 2009). Thus, our data suggest that $Tks5_{short}$ may destabilize invadopodia and interfere with their maturation into a proteolytic state. Hence, the ratio between $Tks5_{short}$ and $Tks5_{long}$, rather than the absolute levels of either isoform or total *Tks5*, appears to be important for invadopodia-mediated cell invasion.

High expression of $Tks5_{long}$ *and low expression of* $Tks5_{short}$ *correlate with metastatic progression and poor survival in lung adenocarcinoma patients*

We next explored whether a high $Tks5_{long}$ to $Tks5_{short}$ ratio correlates with tumor progression and metastasis in human lung cancer. For this purpose, we analyzed RNA sequencing (RNA-seq) data from lung adenocarcinoma patients deposited in The Cancer Genome Atlas (TCGA) for the expression ratio of $Tks5_{long}$ to $Tks5_{short}$. The human $Tks5_{short}$ transcript homologous to mouse $Tks5_{short}$ was the most abundant isoform alternative to $Tks5_{long}$ in these lung tissues (data not shown), although additional transcripts with slight variations exist in other tissue types (S. Courtneidge, pers. comm.; http://genome.ucsc.edu, assembly GRCh37/hg19, gene *Sh3pxd2a*). Importantly, while the expression patterns of $Tks5_{long}$ and $Tks5_{short}$ in these lung adenocarcinomas were diverse, there was a trend toward high $Tks5_{long}$ to $Tks5_{short}$ expression ratios in patients with stage III and IV disease (characterized by metastatic invasion in the thoracic cavity and distant organs, respectively; $n = 59$) compared with patients with stage IA disease (characterized by a single, small, localized lesion without detectible metastases; $n = 57$; $P < 0.009$ by χ^2 test and $P < 0.013$ by Fisher's exact test) (Fig. 6A), suggesting that high $Tks5_{long}$ and low $Tks5_{short}$ expression contributes to promoting metastatic progression.

In addition, we examined $Tks5_{long}$ and $Tks5_{short}$ expression in an independent cohort of 102 patients with stage I/II lung adenocarcinoma from the University of Michigan. Interestingly, we observed that higher $Tks5_{long}$ expression and lower $Tks5_{short}$ expression correlated with worse disease-free survival and overall survival by Kaplan-Meier analysis (Fig. 6B; Supplemental Fig. S5) and reflected poor prognosis in a multivariate analysis by the Cox proportional hazard model after adjustment for gender, age, stage, and tumor differentiation state (Table 1; Supplemental Table S1). Importantly, total expression of *Tks5* did not demonstrate any survival correlation or prognostic values in these analyses (Fig. 6B; Table 1; Supplemental Fig. S5; Supplemental Table S1), suggesting that the distinction between *Tks5* isoforms is critical in analyzing these clinical data. As disease-free survival and, to a lesser extent, overall survival reflect the rate of post-resection tumor relapse and thus, most likely, the magnitude of early micrometastatic spread prior to surgery, our data are consistent with the conclusion that $Tks5_{long}$ promotes metastasis in human lung cancer, while $Tks5_{short}$ exerts the opposite effect, and a shift in the balance of the two isoforms may influence the clinical outcomes in lung adenocarcinoma patients. In addition, $Tks5_{long}$ and $Tks5_{short}$ may serve as prognostic factors for identifying high-risk patients with early stage disease who may benefit from adjuvant treatment following tumor resection.

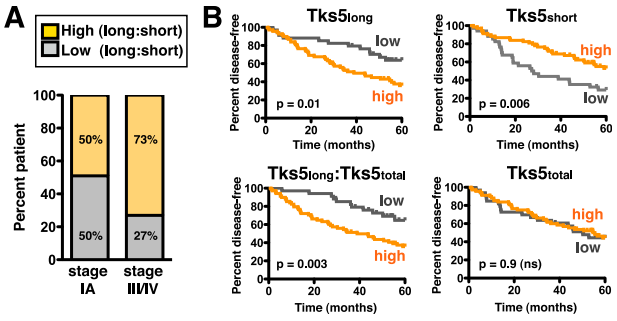

Figure 6. A high $Tks5_{long}$ to $Tks5_{short}$ ratio correlates with metastasis and poor survival in lung adenocarcinoma patients. (*A*) Ratio of $Tks5_{long}$ to $Tks5_{short}$ expression in primary lung adenocarcinomas of stage IA patients ($n = 57$) and stage III/IV patients ($n = 59$). *P*-value < 0.009, χ^2 test; $P < 0.013$, Fisher's exact test, two-tailed. (*B*) Five-year disease-free survival of stage I/II lung adenocarcinoma patients correlates with $Tks5_{long}$ and $Tks5_{short}$ expression but not total expression of *Tks5*. Patients ($n = 102$) were divided into two groups based on expression level (high, top two-thirds; low, bottom one-third). All *P*-values are from log-rank test.

Table 1. *Hazard ratios from multivariate Cox-model analysis of 5-yr disease-free survival*

	Hazard ratio (95% CI)	*P*-value
$Tks5_{long}$	2.1 (1.4–3.2)	0.0003
$Tks5_{short}$	0.5 (0.4–0.8)	0.006
$Tks5_{long}$:$Tks5_{total}$	3.0 (1.6–5.9)	0.0009
$Tks5_{total}$	1.1 (0.8–1.7)	0.5 (ns)

Analysis was adjusted to age, gender, stage, and differentiation. (CI) Confidence interval; (ns) not significant.

Discussion

Metastasis accounts for the vast majority of cancer related deaths, underscoring the need for a better understanding of the molecular mechanisms that enable tumor cells to escape from their primary site and spread to other parts of the body. In this study, we report a shift in the isoform expression of an invadopodia component, *Tks5*, that helps explain the increased invasiveness of metastatic cells during lung adenocarcinoma progression. Our data indicate that as primary tumors progress from a non-metastatic state (T_{nonMet}) to a metastatic state (T_{Met}) and eventually form secondary lesions (Met), tumor cells acquire an increase in $Tks5_{long}$ to $Tks5_{short}$ expression, despite a lack of significant increase in total *Tks5* expression. Using functional experiments in cultured cells and mouse models, we demonstrate distinct and opposing roles for $Tks5_{long}$ and $Tks5_{short}$. $Tks5_{long}$ promotes invadopodia activity and metastasis formation, as knockdown of $Tks5_{long}$ impairs invadopodia function in vitro and metastasis formation in vivo, while elevated expression of $Tks5_{long}$ has the opposite effects. $Tks5_{short}$, on the other hand, acts as a negative regulator of invadopodia function, as increased expression of $Tks5_{short}$ interferes with invadopodia stability and inhibits gelatin proteolysis. Hence, it is the balance of $Tks5_{long}$ and $Tks5_{short}$ expression, rather than total *Tks5* level, that appears to be important for metastatic invasion. Consistent with these functional analyses, our clinical data demonstrate that a high level of $Tks5_{long}$ expression and a low level of $Tks5_{short}$ expression (but not total *Tks5* expression) correlate with

metastatic progression in lung adenocarcinoma patients and predict poor survival of patients with early stage disease.

These experiments provide insight into the roles of *Tks5* isoforms in metastasis. Previous studies have demonstrated a role of *Tks5* in invadopodia and invasion (Seals et al. 2005; Blouw et al. 2008); however, the specific roles of its isoforms have not been defined. Our data revise the current notion that *Tks5* generally promotes invadopodia and metastasis and support a model in which $Tks5_{long}$ acts to promote invadopodia formation by binding to the cellular membrane and recruiting effector proteins for actin polymerization and protease secretion, while $Tks5_{short}$ acts to regulate invadopodia function by interfering with their stability and maturation. A shift in the balance of $Tks5_{long}$ *and* $Tks5_{short}$ expression in cancer cells may have a profound impact on tumor progression. While our data indicate that $Tks5_{short}$ interferes with invadopodia stability, the specific mechanism of this regulation remains to be elucidated. It is conceivable that $Tks5_{short}$ acts by sequestering invadopodia components away from the cell membrane via its multiple SH3 domains, proline-rich regions, and phosphorylation sites. Previous biochemical assays have shown that these functional domains of Tks5 bind to multiple invadopodia components, including N-WASP, Nck, and ADAM family metalloproteases (Abram et al. 2003; Oikawa et al. 2008; Stylli et al. 2009). Whether these protein interactions mediate the inhibitory function of $Tks5_{short}$ in invadopodia deserves future investigation. In addition, given the differential isoform expression of *Tks5* in metastatic and nonmetastatic tumors, it will be of great interest to identify the regulatory mechanism of this isoform switch. Preliminary data from our 5′ RACE and H3K4me3 ChIP-seq analyses suggest that the two isoforms are transcribed from distinct promoters (C Li, unpubl.). Future work will dissect the regulatory mechanisms of promoter choice that lead to the increased expression of $Tks5_{long}$ during tumor progression.

This study also underscores the in vivo role of invadopodia as critical mediators of metastasis in natural tumor progression. While previous studies have provided important evidence for a role of invadopodia in mediating metastatic invasion by using cell culture-based invasion assays and transplant models (Seals et al. 2005; Blouw et al. 2008; Philippar et al. 2008; Eckert et al. 2011; Gligorijevic et al. 2012), these experimental systems often do not fully recapitulate natural tumor progression and metastatic spread. Here we further establish the role of invadopodia in promoting metastasis in vivo by using an autochthonous mouse model of metastatic lung cancer. Our data thus help address the question of whether invadopodia play a physiologically relevant role in metastasis in vivo (Linder 2009; Sibony-Benyamini and Gil-Henn 2012). The data presented by our study and others provide a mechanism that explains one of the ways in which tumor cells might overcome the multiple physical barriers presented by stromal tissues, the extracellular matrix, and endothelial cells during the intravasation, extravasation, and colonization steps of metastasis. Interestingly, while the gain of $Tks5_{long}$ expression in both T_{Met} and Met cells in our lung adenocarcinoma model suggests that invadopodia function in both the invasion/intravasation step at the primary tumor and the extravasation/colonization step at the metastatic site, the specific contribution of invadopodia to each step of the metastasis cascade may be context-dependent and cell type-dependent. Whereas knockdown of $Tks5_{long}$ in lung adenocarcinoma cells (this study) and knockdown of total *Tks5* in Ras-transformed mammary epithelial cells (Eckert et al. 2011) diminished the number of metastases formed, similar total *Tks5* knockdown experiments in Src-transformed mouse embryonic fibroblasts did not lead to more metastases but an increase in the volume and vascularization of metastatic nodules (Blouw et al. 2008). Thus, the specific contribution of invadopodia to each step of the invasion–metastasis cascade in different cancer types remains to be further dissected in the future.

In addition, this study carries clinical implications for lung cancer patients. Previous clinical studies of another invadopodia component, cortactin, indicate that its elevated expression and dysregulated cellular localization correlate with poor survival in laryngeal carcinoma and lung adenocarcinoma, respectively, underlining the relevance of invadopodia activity in predicting clinical outcomes (Gibcus et al. 2008; Hirooka et al. 2011). Consistent with these studies, our data show that a high level of $Tks5_{long}$ expression and a low level of $Tks5_{short}$ expression correlate with metastatic progression of lung adenocarcinoma patients and predict poor survival of patients with early stage disease, suggesting that the $Tks5_{long}$ to $Tks5_{short}$ ratio may serve as a prognostic marker for assessing the metastatic potential of primary tumors and for identifying early stage patients who bear higher risks for metastasis and may benefit from adjuvant therapy after tumor resection. Furthermore, future development of molecular therapeutic strategies that inhibit $Tks5_{long}$ function or strengthen $Tks5_{short}$ activity could potentially help inhibit metastatic progression.

Finally, this study demonstrates the value of mouse models and their derivative cell lines in allowing molecular characterization of the cell state changes that accompany tumor progression and metastasis and is representative of recent developments of animal models for lung adenocarcinoma (Jackson et al. 2005; Politi et al. 2006; Dankort et al. 2007; Ji et al. 2007). Importantly, our approach demonstrates that in order to fully understand the metastatic process, analysis of gene expression at the isoform level in addition to the total gene expression level is important. Given the lethal effects of the metastatic phase of cancer, a deeper insight into the molecular determinants of metastasis will have a significant impact on cancer mortality and morbidity.

Materials and methods

Cell lines

T_{nonMet}, T_{Met}, and Met cell lines were derived from autochthonous tumors in *K-ras*$^{LSL\text{-}G12D/WT}$; *p53*$^{flox/flox}$ mice as described

previously (Winslow et al. 2011). The Massachusetts Institute of Technology Institutional Animal Care and Use Committee approved all animal studies and procedures. Briefly, lung tumors were initiated via intratracheal delivery of a lentiviral vector expressing Cre recombinase. Primary tumors and metastases were harvested at 6–14 mo post-infection and used to establish cell lines. Each metastasis-derived cell line was matched to its primary tumor-derived cell line based on analysis of the unique lentiviral integration site using Southern blotting or linker-mediated PCR. Thus, metastatic primary tumors that had matching secondary lesions could be distinguished from non-metastatic primary tumors. All cell lines were cultured in complete medium (DMEM with 10% FBS, 50 U/mL penicillin, 50 mg/mL streptomycin).

Five T_{nonMet} cell lines (368T1, 393T1, 394T4, 802T4, and 2557T1), six T_{Met} cell lines (373T1, 373T2, 389T2, 393T3, 393T5, and 482T1), and five Met cell lines (373N1, 393N1, 393M1, 482N1, and 482M1) were used for subsequent gene expression analysis and/or functional experiments in this study.

Exon arrays and differential isoform expression detection

Affymetrix GeneChip Mouse Exon 1.0 ST arrays (Gene Expression Omnibus GSE26874) of four T_{nonMet} (368T1, 393T1, 802T4, and 2557T1) and six T_{Met} (373T1, 373T2, 389T2, 393T3, 393T5, and 482T1) cell lines were analyzed for transcriptome-wide isoform switches between groups T_{nonMet} and T_{Met} using the Partek Genomics suite software package (version 6.4) with a custom collection of 345,117 probe sets (~22,000 genes) (Winslow et al. 2011). In summary, Partek data were post-processed using a custom protocol to rank genes based on a combination of (1) statistical significance in Partek's ANOVA-based test for alternative isoform expression, (2) robustly detectible gene expression in both T_{nonMet} and T_{Met} groups, and (3) significant deviation of probe intensity difference between T_{nonMet} and T_{Met} groups for a single probe set, compared with all probe sets of a given gene. High-ranking genes were then further evaluated by manual examination of probe set-based expression profiles in T_{nonMet} and T_{Met} groups.

FITC gelatin degradation assay

Glass-bottomed 35-mm plates (MatTek) were coated with FITC gelatin as described in Bowden et al. (2001) with some modifications. Briefly, MatTek plates were treated with HCl, followed by 50 μg/mL poly-L-lysine, and then coated with a thin layer of FITC-labeled 0.2% gelatin (Sigma) for 1 h. The gelatin coating was then cross-linked with ice-cold 0.8% glutaraldehyde (Electron Microscopy Sciences)/PBS for 15 min at 4°C and then for 30 min at room temperature. Plates were successively washed in PBS (three times for 5 min each), 5 mg/mL sodium borate in PBS (once for 3 min), and PBS (three times for 5 min each), before being incubated for 30 min with complete tissue culture medium. Cells (8×10^4) were cultured on the gelatin-coated plates for 72 h and subsequently processed using standard fluorescence microscopy procedures.

Immunofluorescence staining for invadopodia components

Cells (8×10^4) were grown overnight at 37°C on 35-mm MatTek plates coated with either 0.2% FITC-labeled gelatin or 0.2% plain gelatin (Sigma). Cells were then fixed in 3.7% formaldehyde (Electron Microscopy Sciences) in PBS for 20 min, permeabilized with 0.1% Triton X-100 in PBS for 5 min, and blocked with 1% BSA and 1% FBS in PBS. Subsequently cells were stained for immunofluorescence microscopy. Primary antibodies included Tks5 (1:100; Santa Cruz Biotechnology, M300; detects both $Tks5_{long}$ and $Tks5_{short}$), HA tag (1:100; Cell Signaling, 3724), and cortactin (1:100; Millipore, 4F11). F-actin was stained with phalloidin (Invitrogen).

Live-cell fluorescence microscopy

Cells transfected with a pcDNA3 RFP-β-Actin construct (a generous gift from F. Gertler) were plated on gelatin-coated MatTek dishes in L-15 medium (Leibovitz); placed in an environmental chamber with constant 37°C temperature, CO_2, and humidity; and imaged every 2.5 min for at least 12 h. The lifetimes of at least 150 invadopodia from three independent measurements per condition were analyzed using ImageJ.

Subcutaneous transplant

Nude mice were injected with 5×10^4 T_{Met} cells (393T3 parental cells or 393T3 cells expressing sh1 shRNA against $Tks5_{long}$) resuspended in 100 μL of PBS under the skin on their hind flank. Subcutaneously injected mice were analyzed 8 wk after injection. To quantify lung tumor nodules, all of the visible surface tumors were counted under a dissecting microscope.

Intrasplenic transplant

Nude mice were injected with 5×10^4 T_{Met} cells (373T1 parental cells or 373T1 cells expressing sh1 shRNA against $Tks5_{long}$) resuspended in 200 μL of PBS via the spleen, as described previously (Winslow et al. 2011). Briefly, the animals were given 0.1 mg/kg buprenorphine prior to surgery and anaesthetized with a continuous flow of isoflurane throughout the procedure. Once the animals were under deep anesthesia, the abdominal area was disinfected with betadine and 70% ethanol. The spleen was exposed through a small incision. Cells were injected into the spleen with a single injection using an insulin syringe. Cells were given 10 min to travel through the vasculature to the liver, after which the entire spleen was removed to prevent the formation of a large splenic tumor mass. To remove the spleen, a dissolvable 4-0 suture was tied snugly around the base of the spleen, including the major splenic vasculature, and the spleen was removed. The muscle wall was closed with 4-0 dissolvable sutures, and the skin incision was closed with sterile 7-mm wound clips (Roboz). Intrasplenically injected mice were analyzed 3 wk after injection. Quantification of liver tumor nodules was performed by counting all of the visible surface tumors under a dissecting microscope.

Lentiviral infection of autochthonous mouse model of lung adenocarcinoma

Tumors were initiated by intratracheal infection of mice as described previously (DuPage et al. 2009). Lentivirus was produced from 293T cell transfection as described above. Virus was recovered from the supernatant by ultracentrifugation at 25,000 rpm for 90 min and resuspended in an appropriate volume (200–2000 μL) of PBS. A lentiviral dose of 1000–4000 viral particles induced 25–50 lung tumors per mouse and allowed 6 mo of survival after tumor initiation, while a lentiviral dose of 500 viral particles induced ~10 tumors per mouse and allowed 8 mo of survival post-initiation.

Clinical analysis

For TCGA data set, an index of *Tks5* isoform expression was calculated by [total $Tks5/Tks5_{long}$] based on RNA-seq align-

ments of 305 human lung adenocarcinoma samples (see the Supplemental Material for details). A low value of the index represents a high $Tks5_{long}$ to $Tks5_{short}$ ratio. χ^2 test and Fisher's exact test were performed on patients with stage IA disease (n = 57) and stage III/IV disease (n = 59) using a cutoff of *Tks5* isoform index = 3.6.

For the University of Michigan data set, $Tks5_{long}$ expression and total *Tks5* expression were measured by qRT–PCR in 102 primary tumor samples from patients with stage I/II lung adenocarcinoma. Levels of $Tks5_{short}$ expression were calculated by subtracting $Tks5_{long}$ expression from total *Tks5* expression (see the Supplemental Material for details). Based on expression level, patients were divided into a high-expression group (top two-thirds) and a low-expression group (bottom one-third) for $Tks5_{long}$, $Tks5_{short}$, total *Tks5*, or $Tks5_{long}$ to total *Tks5* ratio. Five-year disease-free survival and overall survival were analyzed by Kaplan-Meier curves and log-rank test. Multivariate analysis by the Cox proportional hazard model (adjusted by gender, age, stage, and tumor differentiation state) was performed using a continuous value of *Tks5* mRNA level to assess survival results. *P*-values (two-tailed) of <0.05 were considered statistically significant.

Acknowledgments

We thank the Swanson Biotechnology Center, and especially Denise Crowley and Eliza Vasile, for technical support. We thank Frank Gertler and Sara Courtneidge for generous sharing of reagents; Angela Brooks and Matthew Meyerson for assistance with TCGA data; Michele Balsamo and Russell McConnell for technical support; Begona Diaz Fernandez for helpful discussions; and Nadya Dimitrova, David Feldser, David McFadden, Thales Papagiannakopoulos, Tuomas Tammela, Wen Xue, Vasilena Gocheva, Irene Blat, Keara Lane, Kim Mercer, Megan Heimann, and the entire Jacks laboratory for advice and experimental assistance. We also thank Phillip Sharp and Frank Gertler for critical reading of the manuscript. This work was supported by a National Institutes of Health grant (5-U01-CA84306) and a National Cancer Institute grant (P30-CA14051). T.J. is a Howard Hughes Investigator, the David H. Koch Professor of Biology, and a Daniel K. Ludwig Scholar. M.M.W. is funded by National Institutes of Health grants (R00-CA151968 and R01-CA175336). C.M.-C.L. is funded by the Ludwig Center for Molecular Oncology Graduate Fellowship. We dedicate this paper to the memory of Officer Sean Collier, for his caring service to the MIT community and for his sacrifice.

References

Abram CL, Seals DF, Pass I, Salinsky D, Maurer L, Roth TM, Courtneidge SA. 2003. The adaptor protein fish associates with members of the ADAMs family and localizes to podosomes of Src-transformed cells. *J Biol Chem* **278:** 16844–16851.

Blouw B, Seals DF, Pass I, Diaz B, Courtneidge SA. 2008. A role for the podosome/invadopodia scaffold protein Tks5 in tumor growth in vivo. *Eur J Cell Biol* **87:** 555–567.

Bowden ET, Coopman PJ, Mueller SC. 2001. Invadopodia: Unique methods for measurement of extracellular matrix degradation in vitro. *Methods Cell Biol* **63:** 613–627.

Bowden ET, Onikoyi E, Slack R, Myoui A, Yoneda T, Yamada KM, Mueller SC. 2006. Co-localization of cortactin and phosphotyrosine identifies active invadopodia in human breast cancer cells. *Exp Cell Res* **312:** 1240–1253.

Chen WT, Olden K, Bernard BA, Chu FF. 1984. Expression of transformation-associated protease(s) that degrade fibronectin at cell contact sites. *J Cell Biol* **98:** 1546–1555.

Clark ES, Whigham AS, Yarbrough WG, Weaver AM. 2007. Cortactin is an essential regulator of matrix metalloproteinase secretion and extracellular matrix degradation in invadopodia. *Cancer Res* **67:** 4227–4235.

Courtneidge SA. 2012. Cell migration and invasion in human disease: The Tks adaptor proteins. *Biochem Soc Trans* **40:** 129–132.

Crimaldi L, Courtneidge SA, Gimona M. 2009. Tks5 recruits AFAP-110, p190RhoGAP, and cortactin for podosome formation. *Exp Cell Res* **315:** 2581–2592.

Dankort D, Filenova E, Collado M, Serrano M, Jones K, McMahon M. 2007. A new mouse model to explore the initiation, progression, and therapy of BRAFV600E-induced lung tumors. *Genes Dev* **21:** 379–384.

DuPage M, Dooley AL, Jacks T. 2009. Conditional mouse lung cancer models using adenoviral or lentiviral delivery of Cre recombinase. *Nat Protoc* **4:** 1064–1072.

Eckert MA, Lwin TM, Chang AT, Kim J, Danis E, Ohno-Machado L, Yang J. 2011. Twist1-induced invadopodia formation promotes tumor metastasis. *Cancer Cell* **19:** 372–386.

Gibcus JH, Mastik M, Menkema L, de Bock GH, Kluin PM, Schuuring E, van der Wal JE. 2008. Cortactin expression predicts poor survival in laryngeal carcinoma. *Br J Cancer* **98:** 950–955.

Gligorijevic B, Wyckoff J, Yamaguchi H, Wang Y, Roussos ET, Condeelis J. 2012. N-WASP-mediated invadopodium formation is involved in intravasation and lung metastasis of mammary tumors. *J Cell Sci* **125:** 724–734.

Hirooka S, Akashi T, Ando N, Suzuki Y, Ishida N, Kurata M, Takizawa T, Kayamori K, Sakamoto K, Fujiwara N, et al. 2011. Localization of the invadopodia-related proteins Actinin-1 and Cortactin to matrix-contact-side cytoplasm of cancer cells in surgically resected lung adenocarcinomas. *Pathobiology* **78:** 10–23.

Jackson EL, Olive KP, Tuveson DA, Bronson R, Crowley D, Brown M, Jacks T. 2005. The differential effects of mutant p53 alleles on advanced murine lung cancer. *Cancer Res* **65:** 10280–10288.

Ji H, Ramsey MR, Hayes DN, Fan C, McNamara K, Kozlowski P, Torrice C, Wu MC, Shimamura T, Perera SA, et al. 2007. LKB1 modulates lung cancer differentiation and metastasis. *Nature* **448:** 807–810.

Kelly T, Mueller SC, Yeh YY, Chen WT. 1994. Invadopodia promote proteolysis of a wide variety of extracellular-matrix proteins. *J Cell Physiol* **158:** 299–308.

Keshamouni V, Arenberg D, Kalemkerian G. 2009. *Lung cancer metastasis: Novel biological mechanisms and impact on clinical practice.* Springer, New York.

Linder S. 2007. The matrix corroded: Podosomes and invadopodia in extracellular matrix degradation. *Trends Cell Biol* **17:** 107–117.

Linder S. 2009. Invadosomes at a glance. *J Cell Sci* **122:** 3009–3013.

Lock P, Abram CL, Gibson T, Courtneidge SA. 1998. A new method for isolating tyrosine kinase substrates used to identify Fish, an SH3 and PX domain-containing protein, and Src substrate. *EMBO J* **17:** 4346–4357.

Murphy DA, Courtneidge SA. 2011. The 'ins' and 'outs' of podosomes and invadopodia: Characteristics, formation and function. *Nat Rev Mol Cell Biol* **12:** 413–426.

Nakahara H, Mueller SC, Nomizu M, Yamada Y, Yeh YY, Chen WT. 1998. Activation of β1 integrin signaling stimulates tyrosine phosphorylation of p190(RhoGAP) and membrane-protrusive activities at invadopodia. *J Biol Chem* **273:** 9–12.

Oikawa T, Itoh T, Takenawa T. 2008. Sequential signals toward podosome formation in NIH-src cells. *J Cell Biol* **182:** 157–169.

Oser M, Yamaguchi H, Mader CC, Bravo-Cordero JJ, Arias M, Chen X, Desmarais V, van Rheenen J, Koleske AJ, Condeelis J. 2009. Cortactin regulates cofilin and N-WASp activities to control the stages of invadopodium assembly and maturation. *J Cell Biol* **186:** 571–587.

Philippar U, Roussos ET, Oser M, Yamaguchi H, Kim HD, Giampieri S, Wang YR, Goswami S, Wyckoff JB, Lauffenburger DA, et al. 2008. A Mena invasion isoform potentiates EGF-induced carcinoma cell invasion and metastasis. *Dev Cell* **15:** 813–828.

Politi K, Zakowski MF, Fan PD, Schonfeld EA, Pao W, Varmus HE. 2006. Lung adenocarcinomas induced in mice by mutant EGF receptors found in human lung cancers respond to a tyrosine kinase inhibitor or to down-regulation of the receptors. *Genes Dev* **20:** 1496–1510.

Rodenhuis S, Slebos RJC, Boot AJM, Evers SG, Mooi WJ, Wagenaar SS, Vanbodegom PC, Bos JL. 1988. Incidence and possible clinical-significance of K-ras oncogene activation in adenocarcinoma of the human-lung. *Cancer Res* **48:** 5738–5741.

Seals DF, Azucena EF, Pass I, Tesfay L, Gordon R, Woodrow M, Resau JH, Courtneidge SA. 2005. The adaptor protein Tks5/Fish is required for podosome formation and function, and for the protease-driven invasion of cancer cells. *Cancer Cell* **7:** 155–165.

Sibony-Benyamini H, Gil-Henn H. 2012. Invadopodia: The leading force. *Eur J Cell Biol* **91:** 896–901.

Siegel R, Naishadham D, Jemal A. 2013. Cancer statistics, 2013. *CA Cancer J Clin* **63:** 11–30.

Stylli SS, Stacey TT, Verhagen AM, Xu SS, Pass I, Courtneidge SA, Lock P. 2009. Nck adaptor proteins link Tks5 to invadopodia actin regulation and ECM degradation. *J Cell Sci* **122:** 2727–2740.

Takahashi T, Nau MM, Chiba I, Birrer MJ, Rosenberg RK, Vinocour M, Levitt M, Pass H, Gazdar AF, Minna JD. 1989. p53: A frequent target for genetic abnormalities in lung-cancer. *Science* **246:** 491–494.

Tarone G, Cirillo D, Giancotti FG, Comoglio PM, Marchisio PC. 1985. Rous-sarcoma virus-transformed fibroblasts adhere primarily at discrete protrusions of the ventral membrane called podosomes. *Exp Cell Res* **159:** 141–157.

Winslow MM, Dayton TL, Verhaak RG, Kim-Kiselak C, Snyder EL, Feldser DM, Hubbard DD, DuPage MJ, Whittaker CA, Hoersch S, et al. 2011. Suppression of lung adenocarcinoma progression by Nkx2-1. *Nature* **473:** 101–104.

Yamaguchi H, Lorenz M, Kempiak S, Sarmiento C, Coniglio S, Symons M, Segall J, Eddy R, Miki H, Takenawa T, et al. 2005. Molecular mechanisms of invadopodium formation: The role of the N-WASP–Arp2/3 complex pathway and cofilin. *J Cell Biol* **168:** 441–452.